

# **Methodology for Enhancing and Evaluating Geologic Effects of Time Series Models: A Case of Ground Response in Santa Clara Valley, California\***

**Olusola Samuel-Ojo<sup>1</sup>, Lorne Olfman<sup>2</sup>, Linda A. Reinen<sup>4</sup>, Arjuna Flenner<sup>3</sup>, David D. Oglesby<sup>5</sup>, and Gareth J. Funning<sup>5</sup>**

Search and Discovery Article #41097 (2012)

Posted December 32, 2012

\*Adapted from extended abstract prepared in conjunction with poster presentation at AAPG International Convention and Exhibition, Singapore, 16-19 September 2012, AAPG©2012

<sup>1</sup>School of Information Systems and Technology, Claremont Graduate University, Claremont, CA ([osamuelojo@yahoo.com](mailto:osamuelojo@yahoo.com))

<sup>2</sup>School of Information Systems and Technology, Claremont Graduate University, Claremont, CA

<sup>3</sup>School of Mathematical Sciences, Claremont Graduate University, Claremont, CA

<sup>4</sup>Geology Department, Pomona College, Claremont, CA

<sup>5</sup>Department of Earth Sciences, University of California, Riverside, Riverside, CA

## **Abstract**

Unlike cross-sectional data models of geologic properties where datasets of regionalized (random) variables take levels (values) that are ‘frozen’ in time, time series data models pose unique characteristics and require special enhancement in order to get the most out of them. Using the groundwater and remote sensing field data between 1992 and 2000 of Santa Clara Valley, USA, we investigate liquefaction deformation, a groundwater-induced ground response. We examine the uniqueness of hydrogeologic (hydraulic heads) and geodetic (PS-InSAR) time series data, and fashion a methodology that enables local and regional geologic features to be more pronounced so that they are better identified and interpreted.

A time series three-phase methodology consisting of disaggregation, application, and aggregation phases is proposed. In the disaggregation phase, observational data are partitioned into inliers and outliers. The inliers are de-noised and decomposed into four main components: levels, trends, cycles, and residuals. In the application phase: parametric and non-parametric quantitative methods are applied, training and validating datasets, local (shallow) and regional (deep), level and residual models are built. These models constitute threads, a computer executable unit that can concurrently be processed by server clusters to achieve high performance results. Levels and residuals are recombined in the aggregation phase in order to make subsurface prediction. The predictive performances of different smoothing techniques are compared by performing a ten-fold cross-validation experiment.

Using the methodology, we produced sixteen models of interaction between groundwater and surface deformation. We also generated from the models, enhanced regional hydraulic head, local direction, velocity, path of groundwater flow isoline maps, describing the hydrogeology variation and ground response in the study area. In a reservoir media consisting of sandstones (solid phase), empty pores (air phase), and filled pores (liquid phase) such as an aquifer, we found that enhanced feature-based time series models produce better plausible results incorporating environmental uncertainties. Resource managers, geoscientists and engineers are likely to use the maps to monitor groundwater volumetric flow for water budget and predict hydraulic conductivity of the aquifer storage for land use. They may use the methodology to monitor other reserves including ores and petroleum as well.

### **Overview**

This study responds to whether trends in surface displacement (deformation) can help in modeling and monitoring short-term fluctuation of the groundwater resource. It processes time series geodetic datasets and hydrogeologic depth-to-water-level readings from wells located in the Santa Clara Valley, CA, USA.

By applying the proposed geospatial information enhancement method consisting of disaggregation, application, and aggregation, the datasets are quality controlled to produce site maps and gain better interpretation of the data.

The regionalized variables including hydraulic head and surface deformation are disaggregated into four data parts: cycle, high frequency, level, and low frequency. The high frequency data part (short-term component) is extracted and mapped. Variations in the high frequency data part are indicative of the short-term changes in groundwater recharge and discharge regime. We produce surface deformation and groundwater subsurface maps and an artificial neural network model of the association between the surface deformation and groundwater potentiometric subsurface, which is able to predict true values.

We concur that that the geodetic data might be preferred to the conventional data obtained from methods that are sometimes labor- and cost-intensive. Resource managers, geoscientists, engineers, data and business analysts might use the proposed method to improve data and model quality in order to gain better understand of the short-term or long-term fluctuation of subsurface resources including groundwater, ore, oil, and gas.

### **Introduction**

In a human lifespan, groundwater is a non renewable resource and should be managed in a sustainable manner taking advantage of spatially extensive and non-invasive methods. Groundwater represents approximately 20% of all fresh water on Earth and in the USA, about 40% of all fresh water comes from groundwater resource (Renton, 2006). When we exploit groundwater for purposes such as

drinking, irrigation, and industrial use, there are possibilities of occurrence of detrimental effects: drying up of wetland, over-pumping, land subsidence, reduction of spring flow, falling groundwater heads, falling well yields, deterioration of water quality, and groundwater pollution.

For a sustainable environmental development of the groundwater system therefore, we need to track the inflow (recharge), distribution, and outflow (discharge) of groundwater on a continuous basis. Having a continuous and frequent data on groundwater is critical to studying different abstraction scenarios or remediation measures in terms of groundwater heads, flow lines, changes in recharge conditions, and chemical composition.

Common methods of groundwater monitoring and tracking involve the drilling and development of the observation wells and piezometers. These methods are generally labor intensive and expensive to employ on a larger scale. In this paper we will address how we might model and monitor groundwater system in a cost-effective manner without sacrificing data quality. We will explore trends and patterns in field datasets, and enhance time series data models to get the most out of them.

Unlike cross-sectional data models of geologic properties where datasets of regionalized (random) variables take values that are ‘frozen’ in time, time series data models pose unique characteristics and require special enhancement. Using the groundwater and remote sensing field data from Santa Clara Valley, USA between 1992 and 2000, we investigate trends in surface deformation and potentiometric surface using satellite mapping time series data known as Permanent Scatterer Interferometric Synthetic Aperture Radar (InSAR), and fashion a methodology that enables local and regional geologic features to be more pronounced so that they are better identified and interpreted.

### **Geology of Santa Clara Valley**

The area of interest, Santa Clara Valley was selected because of its proximity to major causes of natural disaster including short-term cyclic loading earthquakes, long-term static and cyclic loading earth systems, and availability of geodetic and hydrogeologic time series data. The valley includes the city of San Jose and numerous smaller cities with a population of 1.7 million people (USCB, 2011). And as the population continues to grow, there will be an increasing pressure on groundwater pumpage.

Faults and rocks are dated to the Cenozoic time period, i.e., as old as about 2 million years ago (Catchings et al., 2007). The valley’s lithologic characterization largely indicates Pleistocene to Holocene clastic of unconsolidated deposits (clay, silt, sand, and gravel) transported from the adjacent mountain ranges and marine sediments, making it susceptible to both short-term and long-term variation of surface deformation and hydraulic heads (Newhouse et al., 2004). See [Figure 1](#).

## Literature Review

In responding to whether trends in surface deformation can help in modeling and monitoring short-term fluctuation of groundwater resource, we consult a number of disciplines for relevant knowledge and current works including Geology and Hydrogeology, Information Systems, and Technology.

Groundwater monitoring activities are organized activities for the continuous measurement of the actual dynamic state of the underground environment, often used for warning and control purposes (UNESCO, 1992). Groundwater monitoring can be categorized into two types: background monitoring and specific monitoring. Background monitoring is a data collection activity that is performed before significant human interference occurs. It is one of the primary means of collecting data required for groundwater management including measurements of heads and chemical composition of groundwater. It entails establishing a network of data collection sites from existing and abandoned wells. Specific monitoring entails data collection and characterization of the transient state of groundwater specifically targeting an aquifer system when it is substantially exploited for particular purposes or when it is expected to be impacted or polluted by seismogenic or anthropogenic activities.

In practice, clusters of piezometers are installed either in a single borehole at different depth or in different boreholes at different depth. Both observation wells and piezometers are developed before use by injecting and abstracting water into and from the well. Observation wells and piezometers are technically less demanding but labor intensive. They should be supported or complemented by geophysical and remote sensing (geodetic) data collection methods.

Remote sensing is defined as the collection and interpretation of information about a target without physical contact with the target (Sabins, 1986). Remote sensing methods are based on the interaction of electromagnetic radiation and target matter, and they provide interesting satellite images and aerial photographs that can be employed to understand the surface of the earth. The availability, distribution, and quality of groundwater as well as its natural flow pattern are largely determined by the characteristics of the climatic conditions and the surface subsoil (Becht, 2004). Thus the interpretation of the surface can be extrapolated to the unseen subsurface.

The interaction of the electromagnetic radiation and ground surface has been an interesting area of study especially the spectral response or pattern of vegetation characteristics and meteorological applications (Belward, 1991; Lagouarde and Brunet, 1993). Remote sensing employs both passive and active sensors for imaging. Examples of active sensors are seismic body and surface waves (seismic traces), Light Detection and Ranging (LiDAR), and Synthetic-Aperture Radar (SAR). SAR signal was first used in the Second World War on a large scale. It has been rapidly developed to gain better image resolution and coherence since then (Curlander and McDonough, 1991). Space-borne SAR instruments and SAR interferometry (InSAR) were developed. InSAR provides geometric fidelity to a millimeter-scale accuracy and is used to produce digital elevation models (DEMs).

For example, a deformation monitoring network is established around the Three Gorges Dam region in China using InSAR for DEM (Wan et al., 2010). DEMs are generated based on the measurement of phase difference between the sensor and target complex radar signals. InSAR however is limited in that the atmospheric phase screen difference between the master and slave images reduces its accuracy. It suffers geometric and temporal decorrelation (Rocca, 2007). Ferretti et al., (2001) proposed Permanent Scatterer InSAR (PS-InSAR) as a solution to address this limitation, a framework for generalizing DEM from multi-interferogram with a wavelet approach. Instead of extracting information from each pixel of an interferogram, PS-InSAR starts out by identifying artificial or natural point-like stable reflectors (permanent scatterers) from the time series of InSAR images. The coherence of the PS enables the millimeter scale accuracy.

The integration of remote sensing, geographic information systems (GIS) and feature-based modeling boosts the study of poroelastic principles, an important principle that relates the interplay of the surface and subsurface. Aquifers are reservoirs and they exhibit both elastic and plastic deformation. King (1892) reported that the water level in a well located near the train station in Whitewater, WI, rose when a train approached and fell when a train left the station. The fluctuation in water level was greater for a heavy freight train than for a light and faster passenger train. Water level surged up as the approaching train compressed the aquifer and stopped. The aquifer expanded, decreasing the pore pressure when the train departed. This non-uniform pore pressure distribution leads to a time-dependent fluid flow according to Darcy's 1856 law. Geertsma (1966) calls the elastic behavior of the reservoirs poroelasticity which is similar to the theory of the elasticity and viscoelasticity of fluid-saturated porous solids.

PS-InSAR is one of the common geodetic remote sensing methods that can be used to study poroelasticity, conduct groundwater exploration and produce aerial photographs to identify favorable features and deposits of groundwater formation. As earlier stated, remote sensing and PS-InSAR in particular provides opportunity to study the area of interest without being encumbered by the expense of building monitoring wells and stations or conducting expensive conventional leveling surveys. In this paper, we investigate how trends in surface deformation as depicted by PS-InSAR dataset can help in monitoring short-term fluctuation of groundwater resource in the Santa Clara Valley.

## **Methodology**

Based on insights from the design science research approach, we formulate a geospatial information method for enhancing and evaluating geologic time series models. The philosophical underpinning of design science approach holds that the knowledge and understanding of a design problem space and its solution space are acquired in the building and application of an artifact (Hevner and Chatterjee, 2010; Hevner et al., 2004). The method is instantiated and applied to our input datasets.

## **Geospatial Information Enhancement Method for Geologic Time Series Data**

The geospatial information enhancement method for geologic time series data consists of three major phases (disaggregation, application, and aggregation) and five major components (data acquisition and loading, data reduction, signal-to-noise enhancement, data parts, and site model output). See [Figure 2](#).

### **Data Acquisition, Quality and Loading Component**

The disaggregation phase starts out with the data acquisition, quality, and loading component. This component takes one-dimension regionalized variable and disaggregate it into its dimensions based on the objective under investigation. In this paper, the input datasets: groundwater hydraulic head is derived from the depth-to-water-level data logger readings in feet with State Plane Coordinate Systems (SPCS CA zone 3), North American Datum of 1983 (NAD83), and active sensor PS-InSAR field data in meters with Universal Transverse Mercator (UTM zone 10), World Geodetic System WGS 84 coordinate and projection systems. Their measurement units, coordinate and projection systems are harmonized for consistency and image registration alignment.

The input datasets are grouped into two main clusters: inliers and outliers using BoxPlot statistics (Zar, 2010). Inliers are data with relatively high probability of closeness while outliers have low probability of closeness. These two clusters are candidates for further exploration. Customarily, the inliers are processed for wanted anomaly detection while outliers are discarded.

The inliers are again logically grouped into XYZT feature classes and loaded to a data warehousing data mart. The data mart is designed based on a star data warehousing schema that models the relationship between a regionalized variable and its time, space and fact entities (Chen, 2006). While loading the data, data integrity check constraints are defined to achieve quality using primary, secondary and alternate keys. These constraints allow the prevention of occurrence of duplicate, incomplete, or incorrect data.

### **Data Reduction Component**

Data reduction ensures that relevant geophysical corrections (such as gravity and pore fluid pressure correction), migration (plumbing), and conversion (scale normalization) are performed. Here, model quality is checked for stationarity (trending), precision, clarity, completeness, consistency, and resolution. The trending or untrending check procedure ensures that the mean content or seasonal mean is constant or zero which is achieved by subtracted the mean content or seasonal mean or both from the inliers.

### Signal-to-noise Ratio Enhancement Component

This component is indicated by the data prisms. Much like how a physical prism splits white light into a rainbow of colors, the Fourier and Wavelet decomposers split input data into data parts. The data parts offer potentials for richer descriptions of underlying geologic processes. The Fourier decomposer implements the Fast Fourier Transform algorithm for Averaging, Laplacian and Laplacian of Gaussian (LoG) filter. Filtering is a procedure that visits each element of the input data and replaces it with the filtered value. Filters employ a convolution tool. Convolution is the operation of replacing each element of an input with a scaled output functions. An averaging convolution of two signals  $f(x)$  and  $g(x)$  is expressed as:

$$z(x; y) = (f * g)(x; y) = \sum_{s=M_1}^{M_2} \sum_{t=N_1}^{N_2} f(x_i - s; y_i - t)g(s; t)$$

where  $[M_1, M_2]$  and  $[N_1, N_2]$  are the domain of the template function in a discrete form.

A Gaussian filter implements first order differencing while a Laplacian filter uses Laplacian operators and implements second order differencing on a Gaussian filter which is also called a Laplacian of Gaussian (LoG) filter. Retaining the coefficient and dropping the derivatives, a 2-D  $(x, y)$  is expressed as:

$$\nabla^2 (g(x; y) * P) = \nabla^2 (g(x; y)) * P$$

$$\begin{aligned} \nabla^2 g(x; y) &= \frac{\partial^2 g(x; y; \frac{3}{4})}{\partial x^2} U_x + \frac{\partial^2 g(x; y; \frac{3}{4})}{\partial y^2} U_y \\ &= \frac{\partial}{\partial x} g(x; y; \frac{3}{4}) U_x + \frac{\partial}{\partial y} g(x; y; \frac{3}{4}) U_y \\ &= \left( \frac{x^2}{\frac{3}{4}} - 1 \right) e^{-\frac{i(x^2+y^2)}{\frac{3}{4}}} + \left( \frac{y^2}{\frac{3}{4}} - 1 \right) e^{-\frac{i(x^2+y^2)}{\frac{3}{4}}} \\ &= \frac{1}{\frac{3}{4}} \left( \frac{x^2+y^2}{\frac{3}{4}} - 2 \right) e^{-\frac{i(x^2+y^2)}{\frac{3}{4}}} \end{aligned}$$

The above expression is again estimated by convolving two Gaussian filters with difference variance (Marr and Hildreth, 1980). This estimation is known as the Difference of Gaussian (DoG) filter.

### Mathematical Theory of Wavelet Decomposition

Let  $g$  represent a highpass (wavelet) filter,  $h$  represent a lowpass (scaling) filter,  $J$  be the total number of scales (octaves),  $j$  be the current octave index,  $N$  be the size of the inputs,  $n$  be the current input index,  $L$  be the width of the filter or the number of taps, and  $k$  be the current wavelet coefficient. Then a continuous wavelet transform function  $W_f(s,t)$  of an input can be written as an inner product of the input function and the wavelet function composed by the scaling function.

$$W_f(s; u) = \int h_f(t); \frac{1}{s} \tilde{A}((t - u)/s) dt$$

This product is a filtering procedure. In discrete form, the scaling function and the wavelet functions are expressed as:

$$\hat{A}(t) = \sum_k \frac{1}{2^j} h[k] \hat{A}(2t - k); \quad \tilde{A}(t) = \sum_k \frac{1}{2^j} g[k] \hat{A}(2t - k)$$

Further,  $g[k]$  and  $h[k]$  are highpass and lowpass filter coefficients. The input transform can be approximated by the discrete form.

### Data Part Component

The application phase comprises the data part components and other data operations required based on the objective in question. The data parts are: cycle, low frequency, level, high frequency. Cycle data describe seasonal short-term or long-term behavior, observable several times within the data. Low frequency data (trend) are changes in the data from one period to another. Levels are casted as edge points of contrast at different scales (of uniform intensity) or intercepts of regression lines. Edge point of contrast consistently defines regions of changing gradient depicting when an underlying physical process changed its operational level. High frequency data are either random variation or variables that are not accounted for. For example, high frequency data reveals local short-term ground movements, characterized by short periods or short wavelength coming from shallow source. We applied the data parts to build an ANN-based model of association between groundwater and surface deformation.



## Site Model Output Component

The site model output component defines the aggregation phase where we use the data parts directly or combine them. The outputs include geological site descriptions, site interpolation, site geophysical model and cartographic map models. They describe situational and futuristic surfaces, profiles, sections and maps of the site.

Having assured the data quality of our inputs using the three-phase method, we created cartographic map models of the site which will be discussed in result section. We implemented an artificial neural network (ANN) to model the association between the surface deformation and the subsurface hydraulic head.

## Artificial Neural Network Computational Procedure

ANNs are models made of highly interconnected group of simulated neurons that process information in parallel and are able to learn in a similar manner to people (Hornik et al., 1989). Before designing the ANN, the regionalized variable (ReV) of interest, surface deformation, and the depth to water level were untrended. The untrending procedure assumes that the seasonal variation in the ReV is proportional to the mean content. Hence only the seasonal trend was removed. We noted that the qqnorm and qqline diagnostic plots were approximately normal for kriged values obtained from trended data whereas kriged values obtained from untrended (constant or zero mean) data do not. Thus we employed the trended data in the implementation of a feed-forward back propagation ANN model and discarded the untrended. The computational implementation is as follows.

The computational procedure of feed forward back propagation artificial neural network entails six steps:

1. Scale the input vector  $x_i$  by normalizing them, randomize both the training and testing dataset and then present it to input neurons.
2. Initialize all weights to small random values both negative and positive. Input vector is fed forward through the network. The linear combination of inputs and first-layer weights ( $v_{ij}$ ) are used to determine whether the hidden neuron activation function  $g(h_j)$  fires or not. The activation functions are known as sigmoid functions with a mathematical S shape. We implemented logistic function or hyperbolic tangent function.

Logistic function is expressed as:

$$g(h_j) = a_j = \frac{1}{1 + e^{-v_{ij} x_i}}$$

Using the logistic sigmoid function, the output of these neurons combined with the second layer weights are employed to determine whether the output neuron activation function  $g(h_k)$  fires or not.

$$g(h_k) = y_k = \frac{1}{1 + e^{-(\sum_j w_{jk} a_j)}}$$

3. The output error  $e_{ok}$  is obtained as the sum of square difference between the network outputs ( $y_k$ ) and the known response values ( $t_k$ ) from the training data set.

$$e_{ok} = (t_k - y_k) y_k (1 - y_k)$$

The hidden layer error  $e_{hj}$  is given by:

$$e_{hj} = a_j (1 - a_j) \sum_k w_{jk} e_{ok}$$

4. The errors in step 3 is fed backwards through the network in order to update the second layer weights using output errors  $e_o$ , and afterwards, the first layer weights using hidden layer error  $e_h$ . These two updating processes are the 'learning' processes. The output layer weights ( $w_{jk}$ ) is updated (learning) using expression with a stabilizing constant  $\lambda$ :

$$w_{jk} = w_{jk} + \lambda e_{ok} a_j$$

The hidden layer weights ( $v_{ij}$ ) is updated (learning) using expression:

$$v_{ij} = v_{ij} + \lambda e_{hj} x_i$$

5. Repeat step 2 until learning stops or after a convergence threshold.  
6. Back-transform the prediction vector into the original scale measurement (by unscale function).

In this research, the feed forward back propagation neural network architecture was implemented for pure spatial data in order to train in a realistic time frame with a lean network. The pure spatial ANN consists of three input nodes (surface deformation data part, UTM x and UTM y), 10 hidden layer nodes and one output node (hydraulic head). R2 libraries including gstat for Kriging deformation values for well location points and nnet for ANN (Pebesma, 2004) were implemented. We performed a ten-fold cross-validation experiment. For each training and testing dataset, record objects are assigned randomly to training and testing. Ten models of subsurface head and deformation were built and evaluated using precision and recall generalization statistics.

## **Result and Discussion**

Three DEMs of the surface deformation are compared. The local displacement are more pronounced and differentiated from the urban effect in the high frequency data part shown in (c) of [Figure 3](#). The DEM and the geology map of the seasonal average of the depth to water level for the month of December of the entire nine years are shown in [Figure 4](#).

We evaluate the results of the ANN-based model of association of the potentiometric subsurface and surface deformation using precision and recall evaluation statistics. The sensitivity of the model is medium indicating that the model is able to predict true values. The model's test surface deformation (left) and the subsurface hydraulic head prediction (right) are shown in [Figure 5](#).

## **Conclusion**

We presented the proposed geospatial information enhancement method for geologic time series data. It is a three-phase method consisting of disaggregation, application, and aggregation. Applying this method to groundwater and PS-InSAR field data acquired from the Santa Clara Valley, CA, USA, we investigated trends in surface deformation and subsurface potentiometric subsurface.

Starting out with the disaggregation phase, observational data were clustered into inliers and outliers. The inliers were decomposed into four main components: cycle, low frequency, level, high frequency. We applied the data parts to build an ANN-based model of association between groundwater and surface deformation which is able to predict true values. We also generated cartographic map models of enhanced regional hydraulic head, describing the hydrogeology variation and ground response in the study area. We produced surface deformation and groundwater potentiometric subsurface maps and a model of the interaction between surface deformation and groundwater potentiometric subsurface.

We argue that the geodetic data might be preferred to the conventional data obtained from methods that are sometimes labor- and cost-intensive. Resource managers, geoscientists, engineers, data and business analysts might use the proposed method to improve data and model quality in order to gain better understand of the short-term or long-term fluctuation of subsurface resources including groundwater, ore, oil, and gas.

## **Selected References**

Becht, R., 2004, Remote sensing techniques for groundwater prospection, *in* V.S. Kovalevsky, G.P. Kruseman, and K.R. Rushton (eds.), *Groundwater studies: An international guide for hydrogeological investigations*: UNESCO, Paris, 430 p.

Belward, A.S., 1991, Spectral Characteristics of Vegetation, Soil and Water in the Visible, Near Infrared and Middle-Infrared Wavelengths, *in* Belward and Valenzuela (eds.), Remote Sensing Applications and GIS for Resources Management in Developing Countries: Kluwer Academic Publishing, Dordrecht, p. 31-54.

Catchings, R.D., 2007, Near-Surface Structure and Velocities of the Northeastern Santa Cruz Mountains and the Western Santa Clara Valley, California, from seismic imaging: USGS Open-File Report 2007-1039, 70 p.

Chen, P.P., 2006, Suggested research directions for a new frontier: Active conceptual modeling: Proceedings, 25: 1.

Curlander, J.C., and R.N. McDonough, 1991, Synthetic Aperture Radar: Systems and Signal Processing: New York: Wiley, 647 p.

Ferretti, A., C. Prati, and F. Rocca, 2001, Permanent scatterers in SAR interferometry: Geoscience and Remote Sensing, v. 39/1, p. 8-20.

Geertsma, J., 1966, Problems of rock mechanics in petroleum production engineering: Proceedings of the 1st Congress, International Society for Rock Mechanics, v. 1, p. 585-594.

<http://www.onepetro.org/mslib/servlet/onepetropreview?id=ISRM-1CONGRESS-1966-099>

Hevner, A.R., and S. Chatterjee, 2010, Design Research in Information Systems: Theory and Practice: New York: Springer, 320 p.

Hornik, K., M. Stinchcombe, and H. White, 1989, Multilayer Feedforward Networks are Universal Approximators: Neural Networks, v. 2/5, p. 359-366.

King, F.H., 1892, Observations and experiments on the fluctuations in the Level and Rate of Movement of Groundwater on the Wisconsin: Washington, D.C., U.S. Dept. of Agricultural, Weather Bureau, Bulletin, v. 5, 75 p.

Lagouarde, J.P., and Y. Brunet, 1993, A Simple Model for Estimating the Daily Upward Longwave Surface Radiation Flux from NOAA-AVHRR data: International Journal of Remote Sensing, v. 14/5, p. 907-925.

Marr, D.C., and E. Hildreth, 1980, Theory of Edge Detection: Proceedings of the Royal Society of London, Series B., Biological Sciences, v. 207/1167, p. 187-217.

Newhouse, M.W., R.T. Hanson, C.M. Wentworth, R.R. Everett, C.F. Williams, J.C. Tinsley, T.E. Noce, and B.A. Carkin, 2004, Geologic, Water-Chemistry, and Hydrologic Data from Multiple-Well Monitoring Sites and Selected Water-Supply Wells in the Santa Clara Valley, California: USGS Scientific Investigations Report 2004-5250, 134 p.

Pebesma, E.J., 2004, Multivariable geostatistics in S: the gstat package: Computers & Geosciences, v. 30, p. 683-691.

Renton, J.J., 2006, The Nature of Earth: An Introduction to Geology: Teaching Co., Chantilly, Virginia, DVD (6).

Rocca, F., 2007, Modeling Interferogram Stacks: Geoscience and Remote Sensing, v. 45/10, p. 3289-3299.

Rocca, F., T. Wang, and M. Liao, 2010, Time Series InSAR Analysis over Three Gorges Region: Techniques and Applications: Saarbrücken: VDM Verlag Dr. Müller, online resource.

Sabins, F.F., 1986, Remote Sensing: Principles and Interpretation: W. H. Freeman & Co, New York, unpaginated.

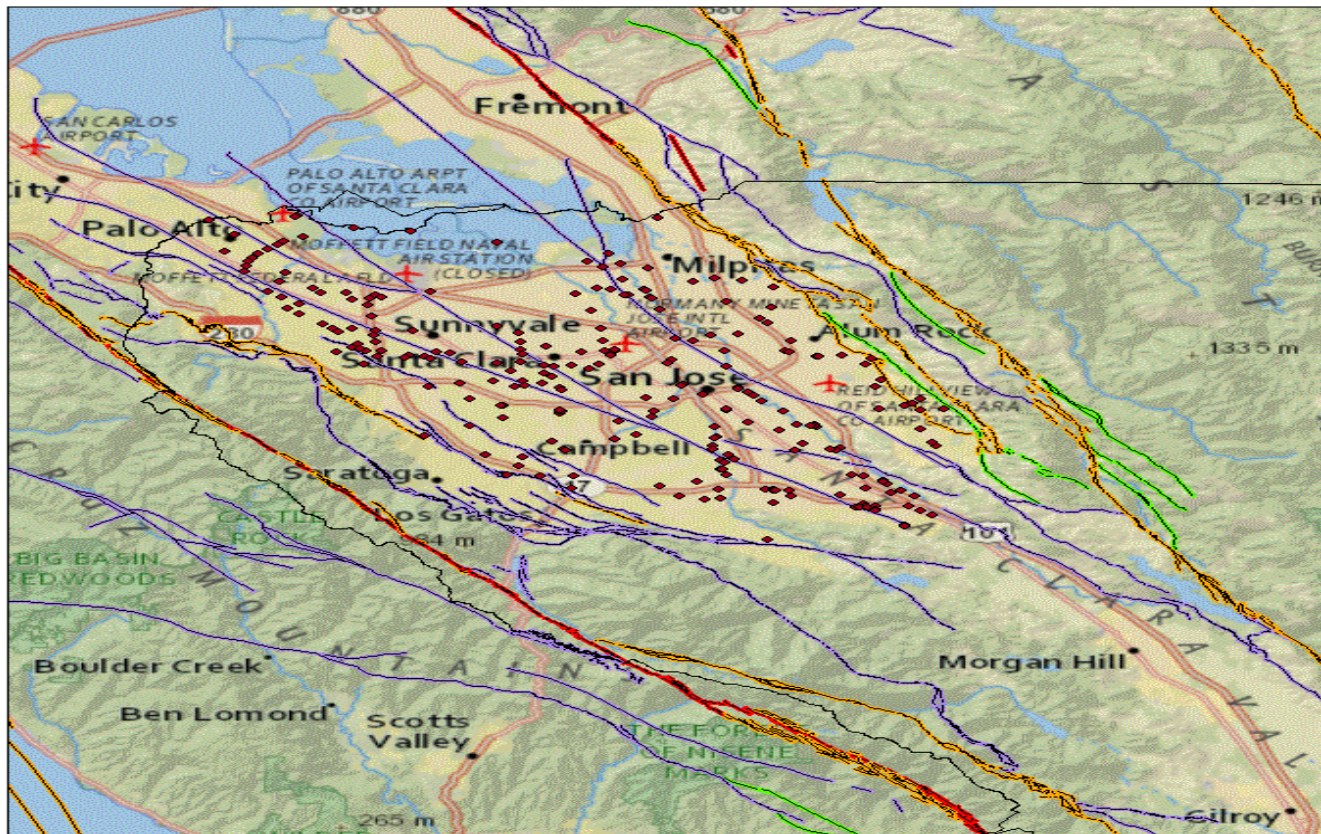
WMO/Unesco Panel on Terminology, 1992, International Glossary of Hydrology: Secretariat of the World Meteorological Organization, 413 p.

Zar, J.H., 2010, Biostatistical Analysis: Prentice Hall/Pearson, Upper Saddle River, N.J., 944 p.

### **Website**

USCB, 2011, Population 2009 Estimate of Santa Clara County, California: US Census Bureau. Web accessed 28 November 2012.  
<http://quickfacts.census.gov/qfd/states/06/06085.html>

Geologic Map of Well and PS-InSAR Observation Locations



0 3,600 7,200 14,400 21,600 28,800 Meters

Red tiny squares indicate the well and PS-InSAR observation locations

Active Fault Symbol	Description
Red line	Historic (<150 yrs)
Orange line	Holocene (<10 ka)
Green line	Late Quaternary (<750 ka)
Blue line	Late Pleistocene (<1.6 ma)
Black line	Early Pleistocene (<2.8 ma)
Grey line	Quaternary (Undifferentiated)
Thin black line	Fault

Figure 1. The geology and location of wells in the Santa Clara Valley, California.

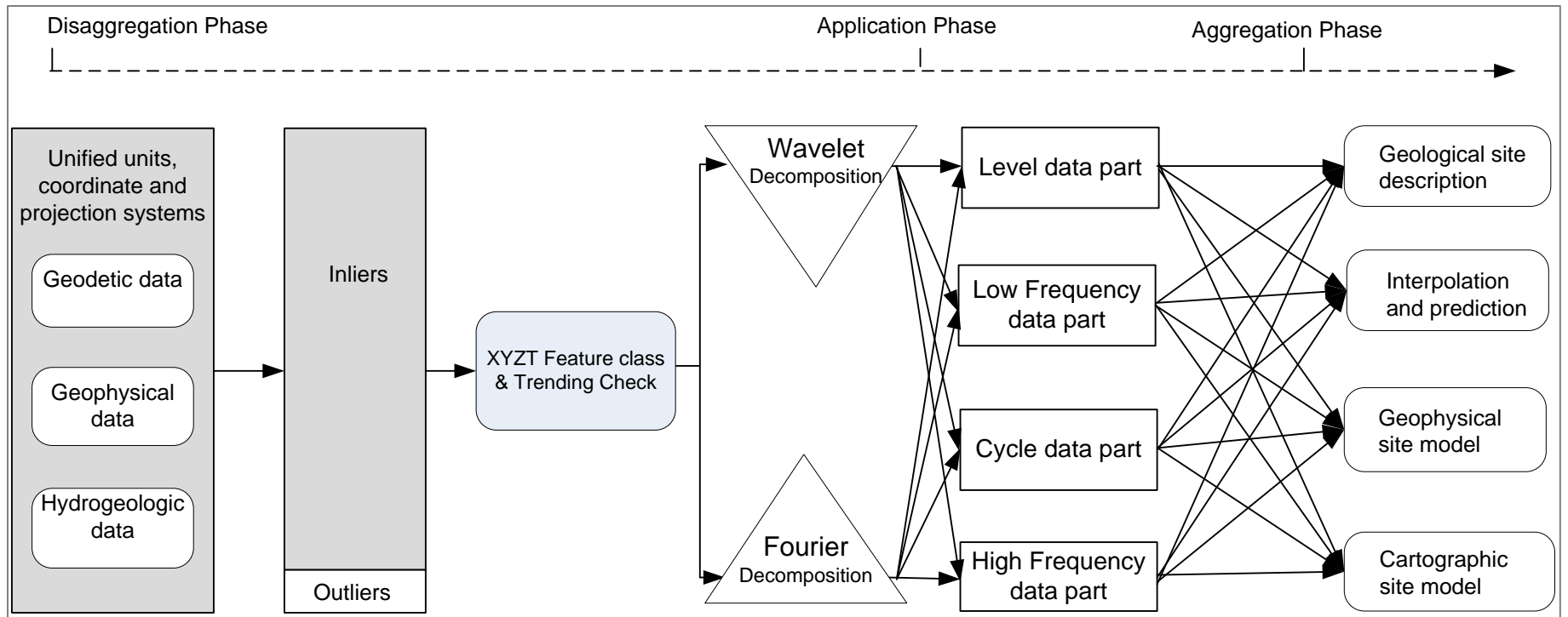


Figure 2. Geospatial information enhancement method for geologic time series data.

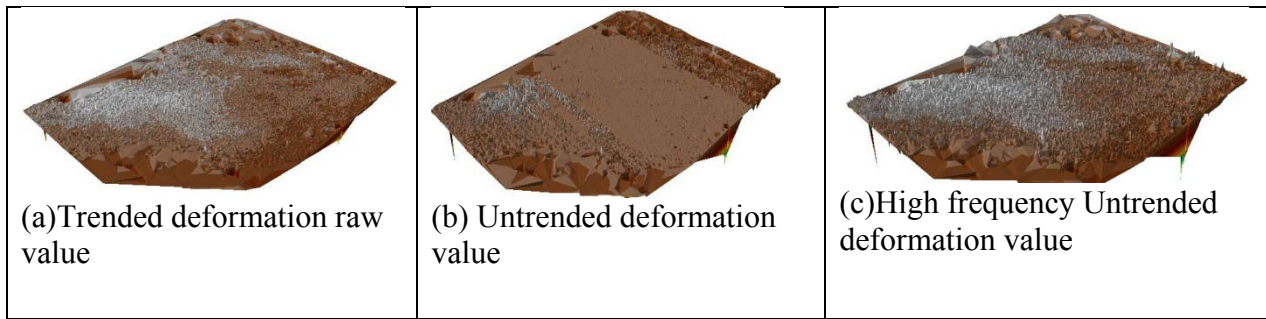


Figure 3. The comparison of three DEMs of the surface deformation (images were produced using (ESRI, 2012)).

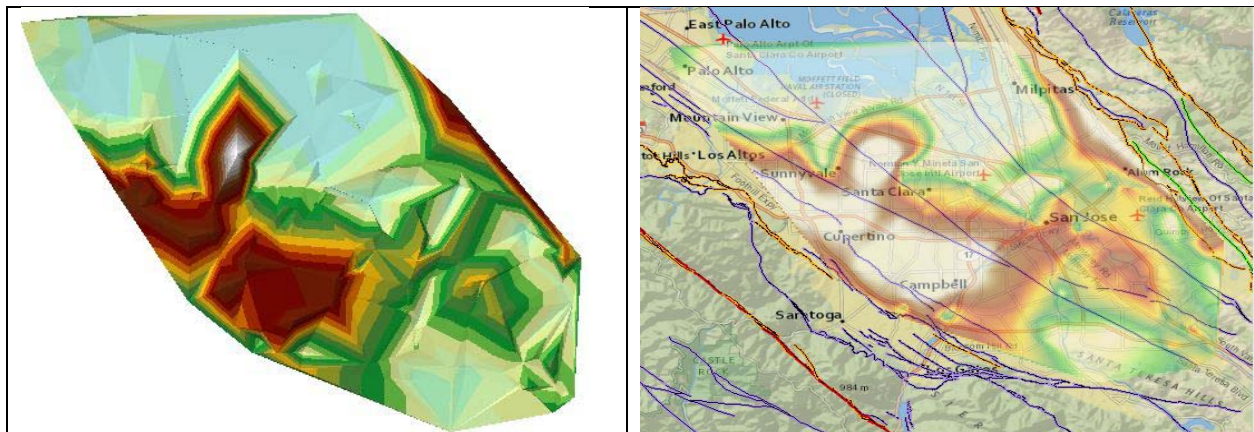


Figure 4. The DEM (left) and the geology map (right) of the seasonal average of the depth to water level for the month of December.



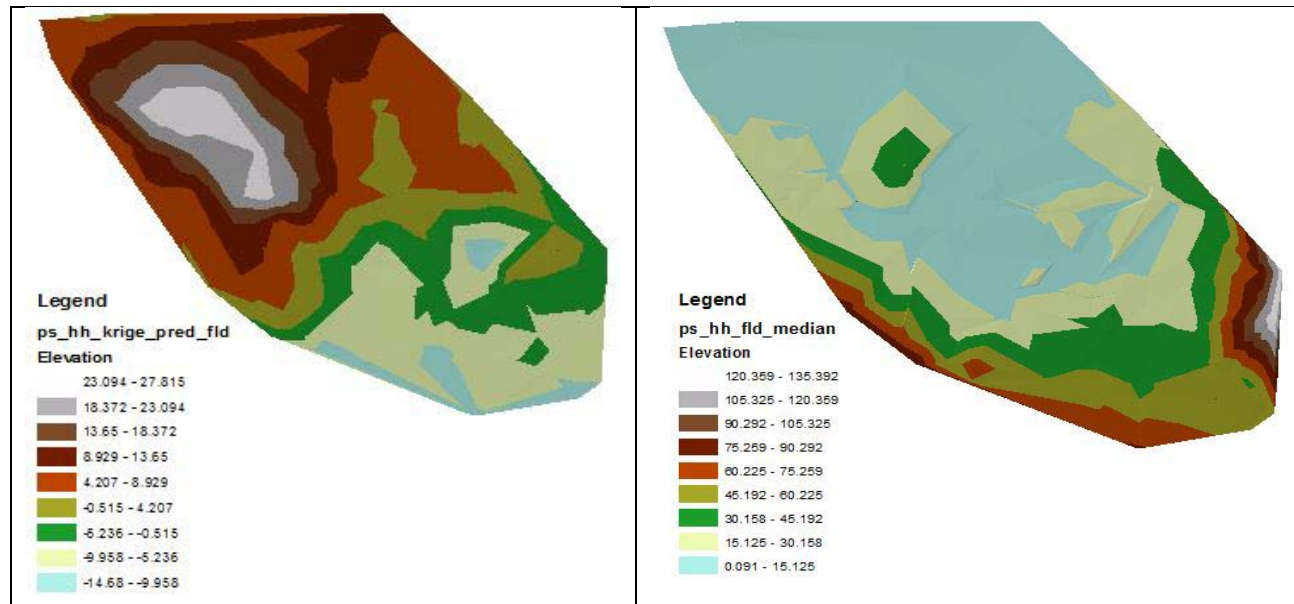


Figure 5. Prediction DEMs of the ANN-based model of surface deformation (left) and the subsurface hydraulic head (right).